

Application of the VUV and the soft x-ray systems on JET for the study of intrinsic impurity behavior in neon seeded hybrid discharges

*Original*

Application of the VUV and the soft x-ray systems on JET for the study of intrinsic impurity behavior in neon seeded hybrid discharges / Krawczyk, N.; Czarnecka, A.; Ivanova-Stanik, I.; Zagórski, R.; Challis, C.; Frigione, D.; Giroud, C.; Graves, J.; Mantsinen, M. J.; Silburn, S.; Subba, F.. - In: REVIEW OF SCIENTIFIC INSTRUMENTS. - ISSN 0034-6748. - 89:10(2018). [10.1063/1.5038930]

*Availability:*

This version is available at: 11583/2986725 since: 2024-03-11T09:29:00Z

*Publisher:*

AMER INST PHYSICS

*Published*

DOI:10.1063/1.5038930

*Terms of use:*

This article is made available under terms and conditions as specified in the corresponding bibliographic description in the repository

*Publisher copyright*

AIP postprint/Author's Accepted Manuscript e postprint versione editoriale/Version of Record

(Article begins on next page)

# Application of the VUV and the soft X-ray systems on JET for the study of intrinsic impurity behavior in neon seeded hybrid discharges<sup>a)</sup>

N. Krawczyk<sup>1,b</sup>, A. Czarnecka<sup>1</sup>, I. Ivanova-Stanik<sup>1</sup>, R. Zagórski<sup>1</sup>, C. Challis<sup>2</sup>, D. Frigione<sup>3</sup>, C. Giroud<sup>2</sup>, J. Graves<sup>4</sup>, M. J. Mantsinen<sup>5,6</sup>, S. Silburn<sup>2</sup> and JET Contributors<sup>c)</sup>

<sup>1</sup>*Institute of Plasma Physics and Laser Microfusion, Hery 23, Warsaw 01-497, Poland*

<sup>2</sup>*CCFE, Culham Science Centre, Abingdon, Oxon, OX14 3DB, UK*

<sup>3</sup>*Associazione EURO-ENEA, C.R.E. Frascati, Italy*

<sup>4</sup>*Centre de Recherches en Physique des Plasmas, EPFL, Lausanne, Switzerland*

<sup>5</sup>*ICREA, Barcelona, Spain*

<sup>6</sup>*Barcelona Supercomputing Center, Barcelona, Spain*

(Presented XXXXX; received XXXXX; accepted XXXXX; published online XXXXX)

Injection of light impurities such as neon (Ne) is one of the technique considered to reduce power load on reactor walls. It could be applied on its own or together with divertor strike-point sweeping in a supporting role<sup>1</sup>. A series of experiments carried out with Ne seeding on JET with the ITER-like-Wall (ILW) suggests increased tungsten release and impurity accumulation as consequences of Ne seeding. For this reason, a detailed study of impurity behaviour together with its control during light gas injection is required. This paper reports on impurity behaviour in a set of hybrid discharges with Ne using the method, which relies mainly on the measurements collected by VUV and soft X-ray diagnostics including the “SOXMOS” spectrometer and the SXR cameras system. Both diagnostics have some limitation. SXR analysis is performed when  $T_e > 1.5\text{-}2\text{ keV}$  and it is not clear what species in the plasma are responsible for this radiation, while VUV due to vertical line of sight (LOS) loses most of tungsten radiation. Consequently, only a combination of measurements from these systems are able to provide comprehensive information about high-Z (e.g. tungsten (W)) and mid-Z (nickel (Ni), iron (Fe), copper (Cu)) impurities for their further quantitative diagnosis. Moreover, thanks to the large number of the SXR LOS, determination of 2D radiation profile was also possible. Additionally, experimental results were compared with numerical modelling based on integrated simulations with COREDIV.

## I. INTRODUCTION

One of the critical issue in the context of future fusion reactors is divertor heat loads limits. In order to reduce excessive heat fluxes to the targets plates, light impurity seeding (using e.g. neon (Ne), nitrogen (N), argon (Ar) or a mixture of them), which are characterized by high radiative loss rate is considered. This approach is of paramount importance especially with a view to a fully metallic device such as ASDEX-Upgrade (W wall and divertor) or JET with the ITER-Like-Wall (ILW with Be limiter and W divertor), or the planned ITER. This is a consequence of the fact that in the case of W and beryllium (Be) plasma facing components (PFCs) the radiation losses that occurs naturally are estimated at low level  $\sim 25\text{-}30\%$  of the heating power, when, for instance, for the carbon elements are at least  $50\%$ <sup>2</sup>. Moreover, for different types

of PFCs, different radiation patterns during Ne seeding are observed. For carbon (C) divertor radiation is mainly located in the SOL and around the X-point, while for W divertor the dominant radiation was found in the plasma core. In considering what an extrinsic impurity as a seeding gas should be applied, such issues like its impact on the plasma confinement and interaction with the PFCs are especially envisaged. In presented study, Ne seeding mainly due to its operational compatibility with the JET tritium handling facility has been chosen<sup>1</sup>. Whereas the injections of light impurities is appropriate for maintaining the power load to the e.g. divertor at an acceptable level, W accumulation is sometimes observed in parallel (depending on electron density and temperature profiles). For this reason, understanding the physics of such effect, as well as, a detailed study of high-, and mid-Z impurity behavior during seeding technique are vital in order to ensure the stability of a plasma.

<sup>a)</sup> Published as part of the Proceedings of the 22nd Topical Conference on High-Temperature Plasma Diagnostics (HTPD 2018) in San Diego, California, USA.

<sup>b)</sup> Author to whom correspondence should be addressed:  
natalia.krawczyk@ifpilm.pl

<sup>c)</sup> See the author list of “X. Litaudon et al Nucl. Fusion **57**, 102001 (2017)”

## II. SETUP OF DIAGNOSTICS FOR IMPURITIES MEASUREMENTS AT JET

Study of W behavior in JET plasmas are realised with a diagnostics combining the soft X-ray (SXR) cameras and a vacuum-ultra-violet (VUV) Schwob-Fraenkel SOXMOS<sup>3</sup> spectrometer, called KT7/3 diagnostic at JET. The first mentioned system consists of horizontal (H) and vertical (V, T) cameras<sup>4</sup>. In the case of presented analysis, only the V-camera, with the large number of lines of sight (LOS) (see FIG.1), were used to determine a W concentration profiles on the basis of a tomographic reconstruction of the registered signals. With this diagnostic, poloidal asymmetries which is caused by centrifugal forces can be obtained as well<sup>5</sup>. Results provided by SXR cameras are based on the assumption that the main radiator is W, while the radiation from other metallic impurities is negligible<sup>5</sup>. To predict the local SXR emissivity due to Bremsstrahlung it is assumed that only Be, and Ne as the low-Z impurities, gives rise to Bremsstrahlung. This is implemented using the effective charge  $Z_{\text{eff}}$  measurements from the visible Bremsstrahlung measurement KS3:ZEFH. Quantitative diagnosis of the W content in this method is described in detail in Ref.<sup>6</sup>. The SOXMOS spectrometer with the 600 g/mm grating is set to record spectra in the wavelength range from 4 to 7 nm. In this spectral region W-ions from  $W^{27+}$  to  $W^{35+}$  are emitted. This particular kind of quasicontinuum, which occurs when the electron temperature lay in the range between 0.8 to 1.8 keV, is used for a quantitative determination of W concentration. Consequently, due to limited radial range, where  $T_e$  is sufficient for proper diagnostic operation, there is some lack of the provided W-content<sup>6</sup>. Therefore, only combining the results from both diagnostics gives the possibility to comprehensive analysis of high-Z impurities behavior. Nevertheless, it needs to be emphasized that the main weakness of presented method is assumption about W and its dominant role in the plasma radiation. It is not exactly clear what species in the plasma have contribution to the soft x-ray radiation, as well as in what quantities. Another important point is that in the case of plasma asymmetry, due to LOS of KT7/3 diagnostic, some part of W radiation can be lost. Because of this, in order to verify the results from W-diagnostics it is also advisable to examine the level of e.g. Ni and other mid-Z impurities, which shall also play a significant role in this kind of analysis. This proposed method should allow to assess the correctness of the assumption about  $Z_{\text{eff}}$  and plasma radiation ( $P_{\text{rad}}$ ). For this purpose the VUV survey spectrometer (known as KT2<sup>6,7</sup> diagnostic at JET), which is mainly intended for the quantitative diagnosis of mid-Z impurities was used. In the wavelength range scanned by the KT2 it is possible to observe different mid-Z impurities like nickel (Ni), iron (Fe), molybdenum (Mo) or copper (Cu). This system equipped with 4500 g/m holographic grating is able to observe the spectrum from 100 to 1100Å, while its spectral resolution is around 5Å. Despite the fact that the best possible time resolution of this diagnostic is 11 ms, the microchannel plate coupled to a 2048 Photo Diode Array

(PDA) usually collects data from 20 to 50 ms time intervals. The relative calibration of this system at short wavelengths is described in Ref.<sup>8</sup>. Moreover, method used for determining mid-Z impurity concentration and  $\Delta Z_{\text{eff}}$  (in steady-state JET plasmas by the use of passive VUV emission), which is based on the Universal Transport Code (UTC) simulations, as well as absolutely calibrated VUV transition intensity measurements is presented in detail by Czarnecka et al. in<sup>9</sup>. For determination of high-Z, and mid-Z impurities concentrations, electron temperature ( $T_e$ ) and electron density ( $n_e$ ) profiles from high resolution Thomson scattering (HRTS) system are taken into account. Setup of discussed diagnostics and their LOS is presented in FIG.1

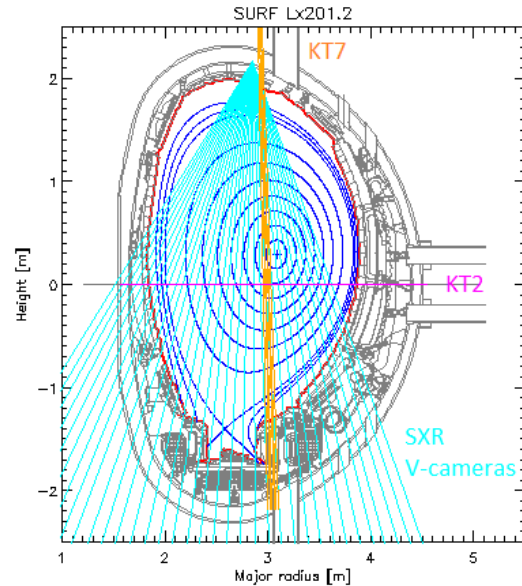


FIG.1. Diagnostic setup for determining mid- and high-Z impurities. The lines of sight of vertical SXR cameras (blue) as well as KT2 (pink) and KT7 (orange) VUV spectrometers with the magnetic equilibrium of JET pulse No: 90337 at 5.75 s.

## III. EXPERIMENTAL AND SIMULATION RESULTS

This work investigates a set of hybrid discharges, where Ne was injected from the divertor region and its rate was changed from pulse to pulse. At the same time other parameters such as the plasma current ( $I_p$ ), magnetic field ( $B_T$ ) and neutral beam injection (NBI) were kept the same at 1.4 MA, 1.9 T and 16.3 MW, respectively. The series of studied discharges consists of 5 pulses with increasing Ne seeding rate (#90336, #90337, #90339, #90279, #90280), as well as reference one, without any injection of external impurity (#90287). Moreover, in all of them additional deuterium gas fueling was equal  $\sim 1.5 \times 10^{22}$  e/s, while a wide region of low magnetic shear with  $q_0 \sim 1$  was created and  $\beta_n$  was limited to  $\sim 2.2$ . Due to the low magnetic field, radio frequency (RF) heating was not applied. For this reason radiative collapse and plasma disruption caused by W accumulation was more likely. Time traces for all selected discharges are presented in FIG.2 The first observation shows that after Ne injection into JET hybrid plasmas, the divertor surface temperature significantly reduced, while radiated power ( $P_{\text{rad}}$ ) and effective charge

( $Z_{\text{eff}}$ ) increased, what is presented in FIG 3. As can be seen, increased W release from PFCs has been observed by SXR cameras system in the core plasma ( $r/a=0$ ) as well as at the mid-radius ( $r/a=0.45$ ). This behavior is not present close to the plasma edge ( $r/a=0.7$ ) as showed data obtained with VUV spectrometer. The presented error bars correspond to an uncertainty of the measured electron densities and temperatures.

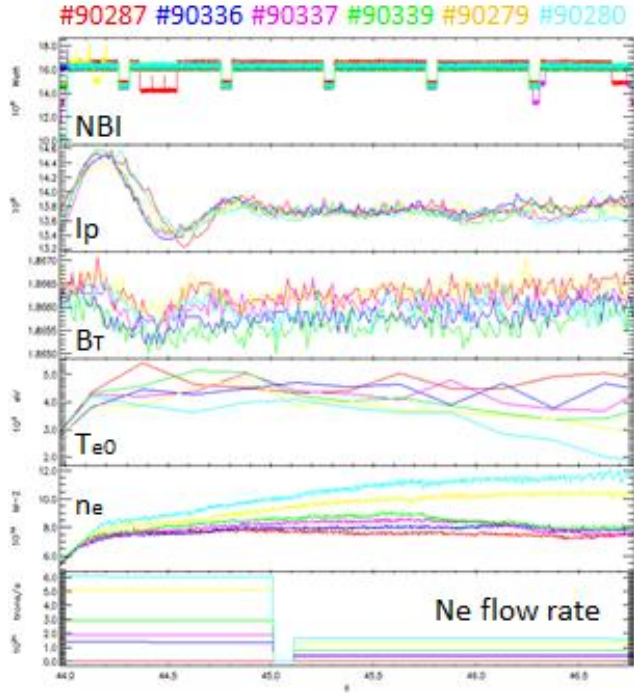


FIG. 2. Time tracers for studied discharges with Ne seeding as well as a reference one.

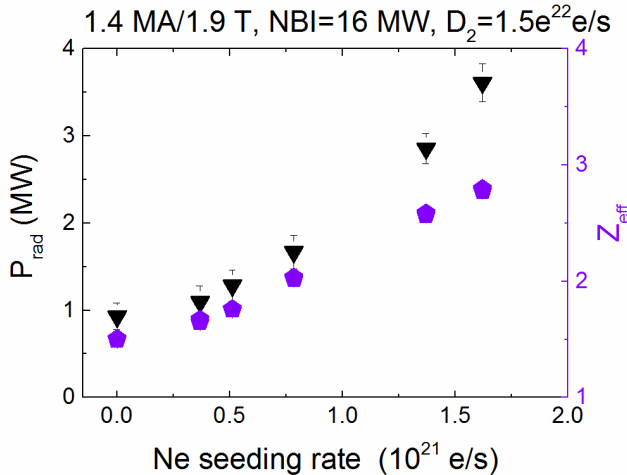


FIG. 3. Radiated power ( $P_{\text{rad}}$ ) for the main chamber only and effective charge ( $Z_{\text{eff}}$ ) versus Ne seeding rate.

Additionally, experimental results were supported by simulations using the COREDIV code<sup>11</sup>. This numerical modeling of plasma parameters solves the 1D radial transport equations of plasma and impurities in the core region and 2D multi-fluid transport in the SOL. In the case

of presented analysis, simulations for the radial diffusion in SOL with  $D_{\text{rad}}^{\text{SOL}} = 0.5 \text{ m}^2/\text{s}$  were carried out. In the core plasma a simply neo-classical model was assumed. The SOL region was approximated by a simple slab geometry (poloidal and radial direction) with classical transport in the poloidal direction and anomalous transport in radial direction using the following transport coefficients  $D_i = \chi_i = 0.5\chi_e$ . Similarly as in the core part of the model, it was assumed that for all ions the anomalous transport is the same and they have the same temperature. What is also important, hybrid discharges selected for this paper were characterized by magnetic configuration with the outer strike point close to the pump out valve (so-called corner configuration). It lead to some implications for the modelling of the W penetration into the plasma. The W atoms which enter the divertor plasma represent only a small fraction of the sputtered ones due to prompt re-deposition processes. Therefore, to reproduce lower radiation, the prompt re-deposition model was included in simulation. In these simulations W source due to sputtering processes (calculated from Ref.<sup>10</sup>) by main ions (D), impurity: seeded (Ne, Ni) and intrinsic (Be) and self-sputtering. As is presented in FIG. 4 experimental results concerning W are consistent with numerical modelling from COREDIV due to the fact that also simulations indicate a noticeable increase in W concentration for the plasma core and mid-radius region. The discussed trend is visible in 2D deconvolutions of SXR signals, as well. Conversely, in the FIG. 5 shows radiated power in the soft x-ray range. Presented reconstructions were carried out for  $t=5.75 \text{ s}$ , while SXR upper range was equal  $25.1 \text{ kW/m}^3$ .

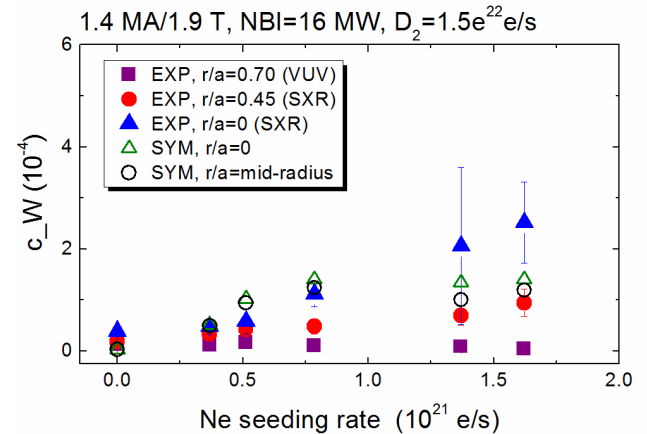


FIG. 4. Comparison of W concentration obtained by SXR system and VUV spectrometer with modelling one based on simulation with COREDIV code for different plasma radius (especially in plasma core and at mid-radius).

At the same time, the rotation velocity resulting from the poloidal in-out asymmetry (observed in the SXR) was compared with that measured by charge exchange recombination spectroscopy (CXRS). This comparison suggest that for higher Ne seeding rate besides of W also Mo is contributing to the SXR radiation. This dependence is also confirmed by measurements provided by VUV spectrometer. FIG. 6 is showing increase of Mo content with Ne seeding rate. It is worth emphasizing that the Mo

as an interlayer in the divertor tiles comes from the same region as W, what can explain their similar behavior during presented experiment.

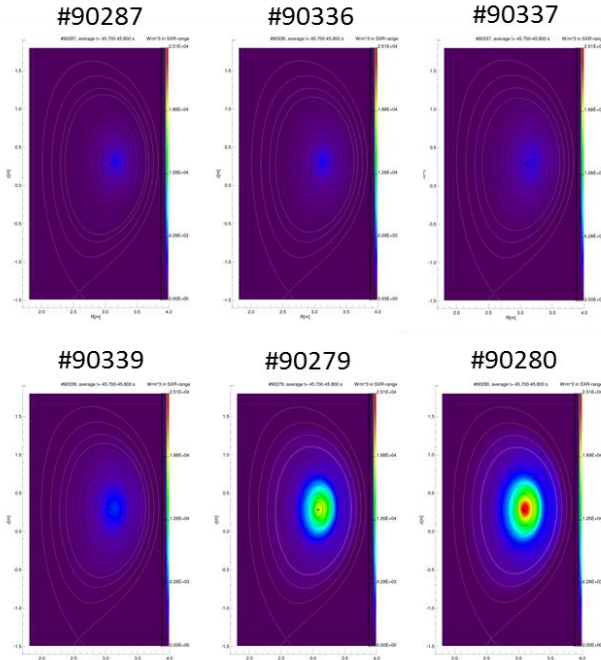


FIG. 5. 2D - profiles of SXR-radiation for set of discharges with Ne seeding obtained from SXR camera system.

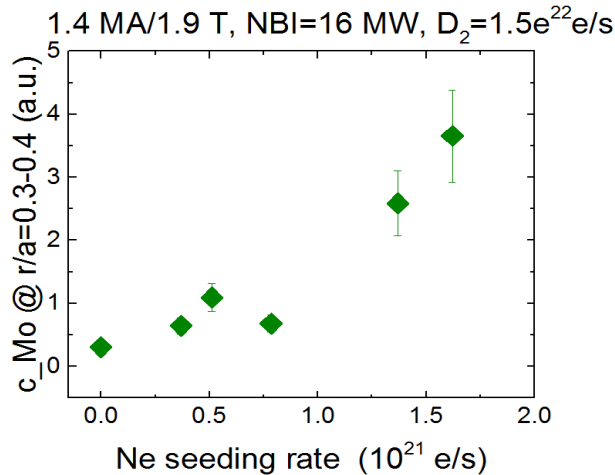


FIG. 6. Mo concentration obtained by VUV spectrometer for plasma region  $r/a=0.3-0.4$

Therefore, on the basis of results concerning W and Mo, it was proved that these impurities can tend to accumulation in the plasma core during light impurity seeding what requires its further observations and control. The different trend is observed for mid-Z impurities such as Ni, Cu and Fe. In the case of Ni, its production comes from structures within the vacuum vessel or is caused by contamination of the plasma facing components. For this reason the effect of Ne seeding on Ni production should be significantly different compared to W and Mo release. As FIG. 7 shows, decrease in Ni intensity line with the increase in Ne seeding rate was observed for plasma region  $r/a=0.3-0.4$ . This trend

obtained from KT2 data was confirmed by simulations, which relies on an assumption that the Ni source is by gas puff in mid plane ( $\Gamma_{Ni}=1.5 \times 10^{19}$  1/s), with recycling coefficient ( $R_{RECYC} = 0.25$ ) and it remains unchanged for all discharges.

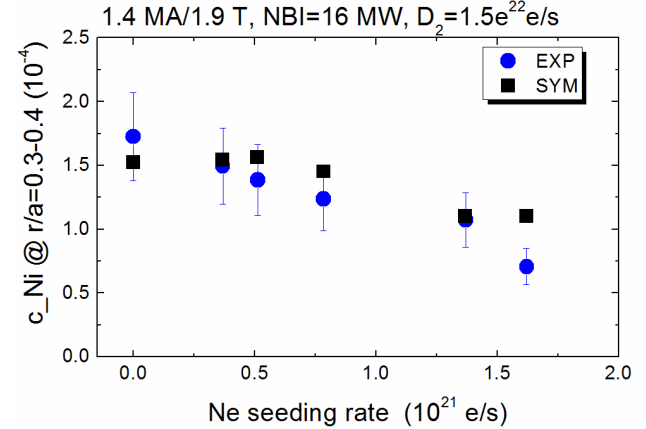


FIG. 7. Comparison of Ni concentration obtained by VUV spectrometer with modelling one based on simulation with COREDIV code for plasma region  $r/a=0.3-0.4$ .

Additionally, total Ni radiation for two marginal discharges – characterized by the lowest (#90336) and the biggest (#90280) amount of injected Ne, have been modeled. FIG. 8 shows this parameter as a function of plasma radius. As in the case of W (see FIG.4), also here it is possible to observe higher radiation on the case of higher seeding. It is due to the fact that for the pulse #90280 we observed higher plasma density ( $n_e$ ) and lower electron temperature ( $T_e$ ) in comparison to #90336. In turn, these two parameters have a significant impact on cooling factor rate, which in addition to plasma volume ( $V$ ),  $n_e$ , and impurity density ( $n_Z$ ) is proportional to calculated Ni radiation.

However, it is worth noting that despite a similar trend for these two types of impurities (high- and mid-Z), the total Ni radiation is an order of magnitude smaller than in the case of W (see FIG.5). Another mid-Z impurities like Fe and Cu behaved in a comparable way such as Ni during studied experiment. Nevertheless, the decreasing tendency is more noticeable for Fe concentration presented in FIG.9. At the same time Cu content presented in FIG. 10, remains more stable with Ne seeding. It can be caused by its different origin – material from the NBI system. Moreover, it is worth emphasizing that in contrast to Ni, Fe and Cu concentrations at plasma radius  $r/a=0.3-0.4$  were very small. It means that they had no significant effect on calculated effective charge. To confirm this assumption, on the basis of data collected by the VUV spectrometer KT2, incremental  $Z_{eff}$  resulting from presented in this paper mid-Z impurities were estimated. As can be seen from FIG.11 incremental effective charge derived from Ni, Fe and Cu are very low. This strengthens results provided by SXR camera system as well as KT7/3, which showed that the increase in  $Z_{eff}$  is dominated by the increase in Ne while the core radiation is dominated by W.

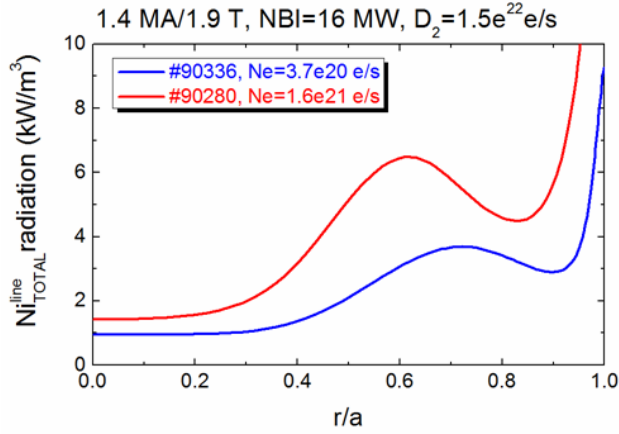


FIG. 8. Comparison of simulated Ni radiation for two discharges with different Ne seeding rate.

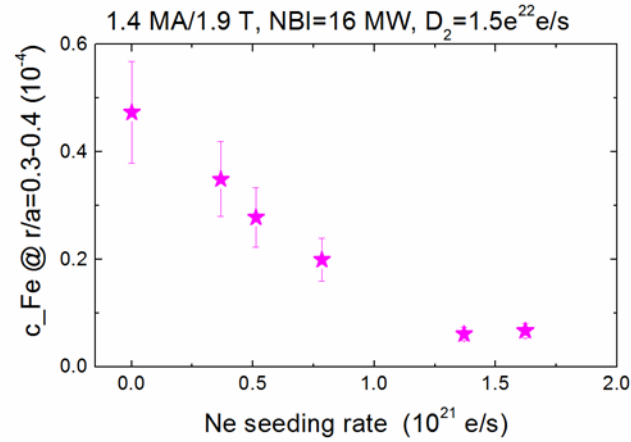


FIG. 9. Iron (Fe) intensity versus Neon (Ne) seeding rate for plasma radius  $r/a=0.3-0.4$  on the basis of data deliver from KT2.

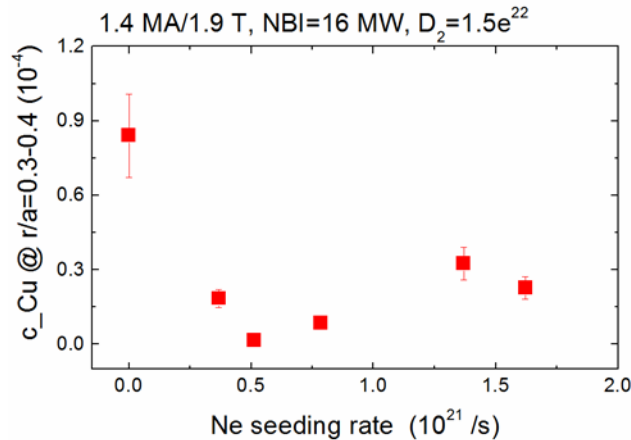


FIG. 10. Copper (Cu) intensity versus Neon (Ne) seeding rate for plasma radius  $r/a=0.3-0.4$  on the basis of data deliver from KT2.

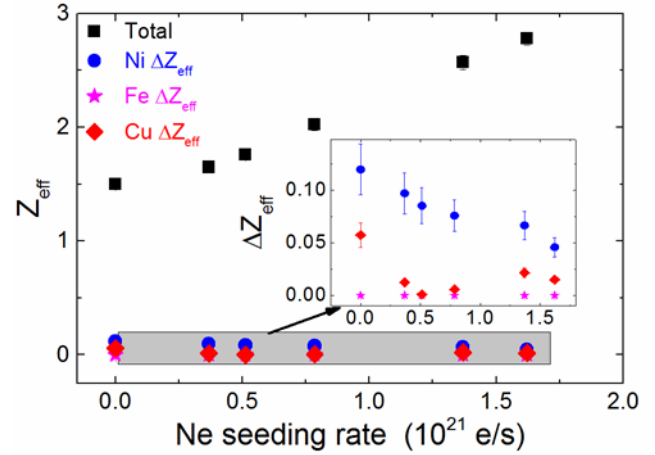


FIG. 11. Incremental  $Z_{eff}$  deliver from Ni, Fe and Cu using VUV diagnostic in comparison on total effective charge  $Z_{eff}$  determined from visible Bremsstrahlung measurements as a function of Ne seeding rate.

#### IV. CONCLUSIONS

The results provided by this paper indicate that Ne seeding technique, which aims to effectively reduce the heat load on the divertor targets requires study related to impurity behavior during such experiments. The proposed method for the evaluation of composition and quantitative diagnosis of impurities confirmed that Ne seeding can lead to increased intrinsic impurity radiation (especially W and Mo) that can have a detrimental effect on plasma performance. In the case of mid-Z impurities like Ni or Fe, with the larger amount of injected gas, their concentration decreased. Moreover, it was found that in comparison with W released, the occurrence of mid-Z impurities was almost negligible. What is also important, results obtained by analysis of the experimental data were consistent with those, which were derived from the simulated one using the COREDIV code.

#### V. ACKNOWLEDGMENTS

This work has been carried out within the framework of the EUROfusion Consortium and has received funding from the Euratom research and training programme 2014-2018 under grant agreement No 633053. The views and opinions expressed herein do not necessarily reflect those of the European Commission. This scientific work was partly supported by Polish Ministry of Science and Higher Education within the framework of the scientific financial resources in the years 2014-2018 allocated for the realization of the international co-financed project.

#### VI. REFERENCES

- <sup>1</sup> C. Challis et al., 2017, Europhysics Conference Abstracts, Vol. 41F, P2.153
- <sup>2</sup> G. Telesca et al Nuclear Materials and Energy **12** (2017)
- <sup>3</sup> J. L. Schwob, A. W. Wouters, S. Suckewer, M. Finkenthal, Rev. Sci. Instrum., **58** 1601 (1987).
- <sup>4</sup> J. Mlynar et al., Soft X-Ray Tomographic Reconstruction of JET ILW Plasmas with Tungsten Impurity and different spectral response of

detectors, Proc. of the 28<sup>th</sup> Symposium on Fusion Technology SOFT, San Sebastian, Spain, 29.09-3.10.2014

<sup>5</sup> T. Putterich et al., Plasma Phys. Control. Fusion **55** 124036 (2013).

<sup>6</sup> T. Putterich et al., Proc. 24rd IAEA Fusion Energy Conf., San Diego, CA 8-13 October 2012 (Vienna: IAEA) vol. IAEA-CN-197, EX-P3.15.

<sup>7</sup> K D. Lawson et al, An absolute sensitivity calibration of the JET VUV SPRED spectrometer, 2009 JINST 4 P04013

<sup>8</sup> A. Czarnecka, et al., This conference

<sup>9</sup> A. Czarnecka, K-D Zastrow, J. Rzedkiewicz, I. H. Coffey, K. D. Lawson, M. G. O'Mullane, Plasma Phys. Control. Fusion **53**, 035009 (2011).

<sup>10</sup> R. Zagorski et al., Modelling with COREDIV Code of JET ILW Configuration, Contrib. Plasma Phys. **50** 306 (2010).

<sup>11</sup> R. Y. Yamamura et al, Institute of Plasma Physics, Nagoya University Report – IPPJ-AM-26.